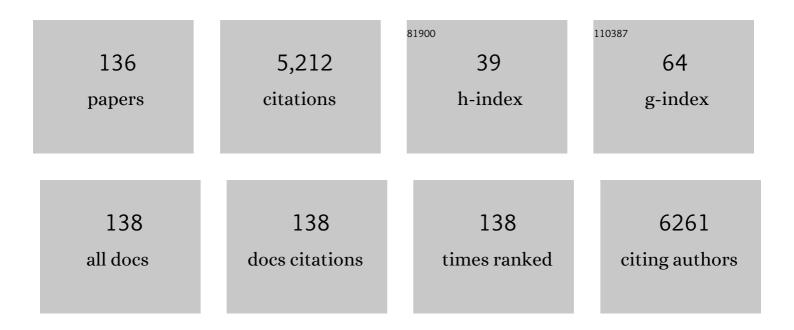


List of Publications by Year in descending order

Source: https://exaly.com/author-pdf/366700/publications.pdf Version: 2024-02-01



LINC LU

#	Article	lF	CITATIONS
1	Endothelial Dysfunction in Atherosclerotic Cardiovascular Diseases and Beyond: From Mechanism to Pharmacotherapies. Pharmacological Reviews, 2021, 73, 924-967.	16.0	359
2	Cardiovascular actions and therapeutic potential of tanshinone IIA. Atherosclerosis, 2012, 220, 3-10.	0.8	295
3	Sirt1 resists advanced glycation end products-induced expressions of fibronectin and TGF-β1 by activating the Nrf2/ARE pathway in glomerular mesangial cells. Free Radical Biology and Medicine, 2013, 65, 528-540.	2.9	223
4	A similarity-based method for prediction of drug side effects with heterogeneous information. Mathematical Biosciences, 2018, 306, 136-144.	1.9	199
5	Electrochemical dual-aptamer-based biosensor for nonenzymatic detection of cardiac troponin I by nanohybrid electrocatalysts labeling combined with DNA nanotetrahedron structure. Biosensors and Bioelectronics, 2019, 134, 49-56.	10.1	132
6	Tanshinone II-A: new perspectives for old remedies. Expert Opinion on Therapeutic Patents, 2013, 23, 149-153.	5.0	122
7	Sensitive electrochemical aptamer cytosensor for highly specific detection of cancer cells based on the hybrid nanoelectrocatalysts and enzyme for signal amplification. Biosensors and Bioelectronics, 2016, 75, 301-307.	10.1	117
8	Tanshinone II A attenuates atherosclerotic calcification in rat model by inhibition of oxidative stress. Vascular Pharmacology, 2007, 46, 427-438.	2.1	98
9	One-Step Electrodeposition of Silver Nanostructures on 2D/3D Metal–Organic Framework ZIF-67: Comparison and Application in Electrochemical Detection of Hydrogen Peroxide. ACS Applied Materials & Interfaces, 2020, 12, 41960-41968.	8.0	90
10	DNA nanotetrahedron-assisted electrochemical aptasensor for cardiac troponin I detection based on the co-catalysis of hybrid nanozyme, natural enzyme and artificial DNAzyme. Biosensors and Bioelectronics, 2019, 142, 111578.	10.1	83
11	H6, a novel hederagenin derivative, reverses multidrug resistance in vitro and in vivo. Toxicology and Applied Pharmacology, 2018, 341, 98-105.	2.8	82
12	Tanshinone II-A inhibits oxidized LDL-induced LOX-1 expression in macrophages by reducing intracellular superoxide radical generation and NF-κB activation. Translational Research, 2012, 160, 114-124.	5.0	78
13	Poly(ADPâ€ribose) Polymerase 1 (PARP1) in Atherosclerosis: From Molecular Mechanisms to Therapeutic Implications. Medicinal Research Reviews, 2014, 34, 644-675.	10.5	77
14	Tanshinone IIA suppresses cholesterol accumulation in human macrophages: role of heme oxygenase-1. Journal of Lipid Research, 2014, 55, 201-213.	4.2	77
15	Aptamer-based electrochemical cytosensors for tumor cell detection in cancer diagnosis: A review. Analytica Chimica Acta, 2019, 1082, 1-17.	5.4	77
16	Tanshinone II-A attenuates and stabilizes atherosclerotic plaques in Apolipoprotein-E knockout mice fed a high cholesterol diet. Archives of Biochemistry and Biophysics, 2011, 515, 72-79.	3.0	76
17	Metal-organic frameworks for improving wound healing. Coordination Chemistry Reviews, 2021, 439, 213929.	18.8	76
18	Cryptotanshinone protects against pulmonary fibrosis through inhibiting Smad and STAT3 signaling pathways. Pharmacological Research, 2019, 147, 104307.	7.1	74

#	Article	IF	CITATIONS
19	SIRT6 suppresses isoproterenol-induced cardiac hypertrophy through activation of autophagy. Translational Research, 2016, 172, 96-112.e6.	5.0	67
20	SESN2 protects against doxorubicin-induced cardiomyopathy via rescuing mitophagy and improving mitochondrial function. Journal of Molecular and Cellular Cardiology, 2019, 133, 125-137.	1.9	67
21	A repeatable assembling and disassembling electrochemical aptamer cytosensor for ultrasensitive and highly selective detection of human liver cancer cells. Analytica Chimica Acta, 2015, 885, 166-173.	5.4	66
22	Competitive electrochemical platform for ultrasensitive cytosensing of liver cancer cells by using nanotetrahedra structure with rolling circle amplification. Biosensors and Bioelectronics, 2018, 120, 8-14.	10.1	66
23	Amelioration of atherosclerosis by tanshinone IIA in hyperlipidemic rabbits through attenuation of oxidative stress. European Journal of Pharmacology, 2012, 674, 359-364.	3.5	63
24	Label-free electrochemical detection of HepG2 tumor cells with a self-assembled DNA nanostructure-based aptasensor. Sensors and Actuators B: Chemical, 2018, 268, 359-367.	7.8	63
25	An Optimized Protocol for Culture of Cardiomyocyte from Neonatal Rat. Cytotechnology, 2005, 49, 109-116.	1.6	61
26	Cryptotanshinone, an orally bioactive herbal compound from <scp>D</scp> anshen, attenuates atherosclerosis in apolipoprotein <scp>E</scp> â€deficient mice: role of lectinâ€like oxidized LDL receptorâ€l (<scp>LOX</scp> â€l). British Journal of Pharmacology, 2015, 172, 5661-5675.	5.4	61
27	Electrochemical biosensor based on gold nanoflowers-encapsulated magnetic metal-organic framework nanozymes for drug evaluation with in-situ monitoring of H2O2 released from H9C2 cardiac cells. Sensors and Actuators B: Chemical, 2020, 311, 127909.	7.8	61
28	TRPM7 is involved in angiotensin II induced cardiac fibrosis development by mediating calcium and magnesium influx. Cell Calcium, 2014, 55, 252-260.	2.4	55
29	Novel Bayesian classification models for predicting compounds blocking hERG potassium channels. Acta Pharmacologica Sinica, 2014, 35, 1093-1102.	6.1	53
30	Cyclovirobuxine D Induces Autophagy-Associated Cell Death via the Akt/mTOR Pathway in MCF-7 Human Breast Cancer Cells. Journal of Pharmacological Sciences, 2014, 125, 74-82.	2.5	51
31	Analysis and Prediction of Nitrated Tyrosine Sites with the mRMR Method and Support Vector Machine Algorithm. Current Bioinformatics, 2018, 13, 3-13.	1.5	51
32	Gene Ontology and KEGG Pathway Enrichment Analysis of a Drug Target-Based Classification System. PLoS ONE, 2015, 10, e0126492.	2.5	50
33	The antihypertensive potential of flavonoids from Chinese Herbal Medicine: A review. Pharmacological Research, 2021, 174, 105919.	7.1	50
34	Roles of transcriptional corepressor RIP140 and coactivator PGC-1α in energy state of chronically infarcted rat hearts and mitochondrial function of cardiomyocytes. Molecular and Cellular Endocrinology, 2012, 362, 11-18.	3.2	48
35	Heme oxygenase-1 ameliorates oxidative stress-induced endothelial senescence via regulating endothelial nitric oxide synthase activation and coupling. Aging, 2018, 10, 1722-1744.	3.1	48
36	NMNAT3 is involved in the protective effect of SIRT3 in Ang II-induced cardiac hypertrophy. Experimental Cell Research, 2016, 347, 261-273.	2.6	44

#	Article	IF	CITATIONS
37	Cryptotanshinone inhibits human glioma cell proliferation in vitro and in vivo through SHP-2-dependent inhibition of STAT3 activation. Cell Death and Disease, 2017, 8, e2767-e2767.	6.3	44
38	α-Enolase plays a catalytically independent role in doxorubicin-induced cardiomyocyte apoptosis and mitochondrial dysfunction. Journal of Molecular and Cellular Cardiology, 2015, 79, 92-103.	1.9	43
39	Autophagy activation attenuates angiotensin II-induced cardiac fibrosis. Archives of Biochemistry and Biophysics, 2016, 590, 37-47.	3.0	43
40	Influence of ferric iron on the electrochemical behavior of pyrite. Ionics, 2011, 17, 169-176.	2.4	41
41	Vps4A mediates the localization and exosome release of β-catenin to inhibit epithelial-mesenchymal transition in hepatocellular carcinoma. Cancer Letters, 2019, 457, 47-59.	7.2	41
42	Cryptotanshinone Attenuates Cardiac Fibrosis via Downregulation of COX-2, NOX-2, and NOX-4. Journal of Cardiovascular Pharmacology, 2014, 64, 28-37.	1.9	40
43	Chrysophanol protects against doxorubicin-induced cardiotoxicity by suppressing cellular PARylation. Acta Pharmaceutica Sinica B, 2019, 9, 782-793.	12.0	40
44	Activation of peroxisome proliferator-activated receptor- \hat{l} ± prevents glycogen synthase $3\hat{l}^2$ phosphorylation and inhibits cardiac hypertrophy. FEBS Letters, 2007, 581, 3311-3316.	2.8	39
45	Bergapten: A review of its pharmacology, pharmacokinetics, and toxicity. Phytotherapy Research, 2021, 35, 6131-6147.	5.8	39
46	Design, synthesis, nitric oxide release and antibacterial evaluation of novel nitrated ocotillol-type derivatives. European Journal of Medicinal Chemistry, 2015, 101, 71-80.	5.5	36
47	Therapeutic effect of Cryptotanshinone on experimental rheumatoid arthritis through downregulating p300 mediated-STAT3 acetylation. Biochemical Pharmacology, 2017, 138, 119-129.	4.4	36
48	SIRT6 suppresses phenylephrine-induced cardiomyocyte hypertrophy though inhibiting p300. Journal of Pharmacological Sciences, 2016, 132, 31-40.	2.5	34
49	Mitochondrial binding of α-enolase stabilizes mitochondrial membrane: Its role in doxorubicin-induced cardiomyocyte apoptosis. Archives of Biochemistry and Biophysics, 2014, 542, 46-55.	3.0	33
50	C/EBPβ knockdown protects cardiomyocytes from hypertrophy via inhibition of p65-NFκB. Molecular and Cellular Endocrinology, 2014, 390, 18-25.	3.2	33
51	G3BP2 is involved in isoproterenol-induced cardiac hypertrophy through activating the NF-κB signaling pathway. Acta Pharmacologica Sinica, 2018, 39, 184-194.	6.1	33
52	Protein kinase CK2α catalytic subunit ameliorates diabetic renal inflammatory fibrosis via NF-κB signaling pathway. Biochemical Pharmacology, 2017, 132, 102-117.	4.4	32
53	The orphan receptor <scp>NOR</scp> 1 participates in isoprenalineâ€induced cardiac hypertrophy by regulating <scp>PARP</scp> â€1. British Journal of Pharmacology, 2015, 172, 2852-2863.	5.4	31
54	Finding Candidate Drugs for Hepatitis C Based on Chemical-Chemical and Chemical-Protein Interactions. PLoS ONE, 2014, 9, e107767.	2.5	31

#	Article	IF	CITATIONS
55	Estimation of acute oral toxicity in rat using local lazy learning. Journal of Cheminformatics, 2014, 6, 26.	6.1	30
56	STAT3 Suppression Is Involved in the Protective Effect of SIRT6 Against Cardiomyocyte Hypertrophy. Journal of Cardiovascular Pharmacology, 2016, 68, 204-214.	1.9	30
57	Identification of new candidate drugs for lung cancer using chemical–chemical interactions, chemical–protein interactions and a K-means clustering algorithm. Journal of Biomolecular Structure and Dynamics, 2016, 34, 906-917.	3.5	30
58	Therapeutic effect of Cryptotanshinone on collagen-induced arthritis in rats via inhibiting nuclear factor kappa B signaling pathway. Translational Research, 2015, 165, 704-716.	5.0	29
59	Sirtuin 1 represses PKCâ€Î¶ activity through regulating interplay of acetylation and phosphorylation in cardiac hypertrophy. British Journal of Pharmacology, 2019, 176, 416-435.	5.4	29
60	JMJD3 inhibition protects against isoproterenol-induced cardiac hypertrophy by suppressing β-MHC expression. Molecular and Cellular Endocrinology, 2018, 477, 1-14.	3.2	29
61	PPARα activation inhibits endothelin-1-induced cardiomyocyte hypertrophy by prevention of NFATc4 binding to GATA-4. Archives of Biochemistry and Biophysics, 2012, 518, 71-78.	3.0	28
62	Estimation of elimination half-lives of organic chemicals in humans using gradient boosting machine. Biochimica Et Biophysica Acta - General Subjects, 2016, 1860, 2664-2671.	2.4	27
63	Design, synthesis, and discovery of ocotillol-type amide derivatives as orally available modulators of P-glycoprotein-mediated multidrug resistance. European Journal of Medicinal Chemistry, 2019, 161, 118-130.	5.5	27
64	COX-2 is involved in ET-1-induced hypertrophy of neonatal rat cardiomyocytes: Role of NFATc3. Molecular and Cellular Endocrinology, 2014, 382, 998-1006.	3.2	25
65	Pharmacological and cardiovascular perspectives on the treatment of COVID-19 with chloroquine derivatives. Acta Pharmacologica Sinica, 2020, 41, 1377-1386.	6.1	25
66	PARP-2 knockdown protects cardiomyocytes from hypertrophy via activation of SIRT1. Biochemical and Biophysical Research Communications, 2013, 430, 944-950.	2.1	23
67	A novel three-dimensional microfluidic platform for on chip multicellular tumor spheroid formation and culture. Microfluidics and Nanofluidics, 2014, 17, 831-842.	2.2	23
68	Salvianolic acid B protects cardiomyocytes from angiotensin II-induced hypertrophy via inhibition of PARP-1. Biochemical and Biophysical Research Communications, 2014, 444, 346-353.	2.1	23
69	Voltammetric aptamer based detection of HepG2 tumor cells by using an indium tin oxide electrode array and multifunctional nanoprobes. Mikrochimica Acta, 2017, 184, 3487-3496.	5.0	23
70	Protocatechuic aldehyde protects against isoproterenol-induced cardiac hypertrophy via inhibition of the JAK2/STAT3 signaling pathway. Naunyn-Schmiedeberg's Archives of Pharmacology, 2018, 391, 1373-1385.	3.0	23
71	SIRT6 Suppresses NFATc4 Expression and Activation in Cardiomyocyte Hypertrophy. Frontiers in Pharmacology, 2018, 9, 1519.	3.5	23
72	ldentifying potential active components of walnut leaf that action diabetes mellitus through integration of UHPLC-Q-Orbitrap HRMS and network pharmacology analysis. Journal of Ethnopharmacology, 2020, 253, 112659.	4.1	23

#	Article	IF	CITATIONS
73	The poly(ADP-ribosyl)ation of FoxO3 mediated by PARP1 participates in isoproterenol-induced cardiac hypertrophy. Biochimica Et Biophysica Acta - Molecular Cell Research, 2016, 1863, 3027-3039.	4.1	22
74	Dkk1 exacerbates doxorubicin-induced cardiotoxicity by inhibiting Wnt/β-catenin signaling pathway. Journal of Cell Science, 2019, 132, .	2.0	22
75	lsorhapontigenin protects against doxorubicin-induced cardiotoxicity via increasing YAP1 expression. Acta Pharmaceutica Sinica B, 2021, 11, 680-693.	12.0	22
76	Bilobalide: A review of its pharmacology, pharmacokinetics, toxicity, and safety. Phytotherapy Research, 2021, 35, 6114-6130.	5.8	22
77	Synthesis and Antibacterial Evaluation of Novel 3-Substituted Ocotillol-Type Derivatives as Leads. Molecules, 2017, 22, 590.	3.8	21
78	PARP1 interacts with STAT3 and retains active phosphorylated-STAT3 in nucleus during pathological myocardial hypertrophy. Molecular and Cellular Endocrinology, 2018, 474, 137-150.	3.2	20
79	Targeting castration-resistant prostate cancer with a novel RORÎ ³ antagonist elaiophylin. Acta Pharmaceutica Sinica B, 2020, 10, 2313-2322.	12.0	20
80	Ginsenosides in central nervous system diseases: Pharmacological actions, mechanisms, and therapeutics. Phytotherapy Research, 2022, 36, 1523-1544.	5.8	20
81	BIG1, a Brefeldin A–Inhibited Guanine Nucleotide-Exchange Protein Modulates ATP-Binding Cassette Transporter A-1 Trafficking and Function. Arteriosclerosis, Thrombosis, and Vascular Biology, 2013, 33, e31-8.	2.4	19
82	MicroRNA-214 contributes to Ang II-induced cardiac hypertrophy by targeting SIRT3 to provoke mitochondrial malfunction. Acta Pharmacologica Sinica, 2021, 42, 1422-1436.	6.1	18
83	The poly(ADP-ribosyl)ation of BRD4 mediated by PARP1 promoted pathological cardiac hypertrophy. Acta Pharmaceutica Sinica B, 2021, 11, 1286-1299.	12.0	18
84	Histone H4R3 symmetric di-methylation by Prmt5 protects against cardiac hypertrophy via regulation of Filip1L/β-catenin. Pharmacological Research, 2020, 161, 105104.	7.1	17
85	Targeting autophagy peptidase ATG4B with a novel natural product inhibitor Azalomycin F4a for advanced gastric cancer. Cell Death and Disease, 2022, 13, 161.	6.3	17
86	Asymmetric Construction of 4 <i>H</i> -Pyrano[3,2- <i>b</i>]indoles via Cinchonine-Catalyzed 1,4-Addition of 2-Ylideneoxindole with Malononitrile. Journal of Organic Chemistry, 2019, 84, 5450-5459.	3.2	16
87	Histone Demethylase JMJD3 Mediated Doxorubicin-Induced Cardiomyopathy by Suppressing SESN2 Expression. Frontiers in Cell and Developmental Biology, 2020, 8, 548605.	3.7	16
88	MicroRNA-34c-5p provokes isoprenaline-induced cardiac hypertrophy by modulating autophagy via targeting ATG4B. Acta Pharmaceutica Sinica B, 2022, 12, 2374-2390.	12.0	16
89	Effectiveness of combination therapy of atorvastatin and non lipid-modifying tanshinone IIA from Danshen in a mouse model of atherosclerosis. International Journal of Cardiology, 2014, 174, 878-880.	1.7	15
90	Effects of ERK1/2/PPARα/SCAD signal pathways on cardiomyocyte hypertrophy induced by insulin-like growth factor 1 and phenylephrine. Life Sciences, 2015, 124, 41-49.	4.3	15

#	Article	IF	CITATIONS
91	Analysis and Identification of Aptamer-Compound Interactions with a Maximum Relevance Minimum Redundancy and Nearest Neighbor Algorithm. BioMed Research International, 2016, 2016, 1-9.	1.9	15
92	sFRP1 has a biphasic effect on doxorubicin-induced cardiotoxicity in a cellular location-dependent manner in NRCMs and Rats. Archives of Toxicology, 2019, 93, 533-546.	4.2	15
93	Preparation of Oral Core–Shell Zein Nanoparticles to Improve the Bioavailability of Glycyrrhizic Acid for the Treatment of Ulcerative Colitis. Biomacromolecules, 2022, 23, 210-225.	5.4	15
94	A fusant of Sphingomonas sp. GY2B and Pseudomonas sp. GP3A with high capacity of degrading phenanthrene. World Journal of Microbiology and Biotechnology, 2013, 29, 1685-1694.	3.6	14
95	Prediction of Cancer Drugs by Chemical-Chemical Interactions. PLoS ONE, 2014, 9, e87791.	2.5	14
96	Microfluidic contactless conductivity cytometer for electrical cell sensing and counting. RSC Advances, 2015, 5, 59306-59313.	3.6	14
97	Machine Learning-Based Modeling of Drug Toxicity. Methods in Molecular Biology, 2018, 1754, 247-264.	0.9	14
98	Sorting nexin 3 induces heart failure via promoting retromer-dependent nuclear trafficking of STAT3. Cell Death and Differentiation, 2021, 28, 2871-2887.	11.2	14
99	PARP1 interacts with HMGB1 and promotes its nuclear export in pathological myocardial hypertrophy. Acta Pharmacologica Sinica, 2019, 40, 589-598.	6.1	13
100	sFRP1 protects H9c2 cardiac myoblasts from doxorubicin-induced apoptosis by inhibiting the Wnt/PCP-JNK pathway. Acta Pharmacologica Sinica, 2020, 41, 1150-1157.	6.1	13
101	Effects of L-leucine on the properties of spray-dried swellable microparticles with wrinkled surfaces for inhalation therapy of pulmonary fibrosis. International Journal of Pharmaceutics, 2021, 610, 121223.	5.2	13
102	Tumor suppressor gene ING3 induces cardiomyocyte hypertrophy via inhibition of AMPK and activation of p38 MAPK signaling. Archives of Biochemistry and Biophysics, 2014, 562, 22-30.	3.0	12
103	Changes in shortâ€chain acylâ€coA dehydrogenase during rat cardiac development and stress. Journal of Cellular and Molecular Medicine, 2015, 19, 1672-1688.	3.6	12
104	PKCζ interacts with STAT3 and promotes its activation in cardiomyocyte hypertrophy. Journal of Pharmacological Sciences, 2016, 132, 15-23.	2.5	12
105	Flavine adenine dinucleotide inhibits pathological cardiac hypertrophy and fibrosis through activating short chain acyl-CoA dehydrogenase. Biochemical Pharmacology, 2020, 178, 114100.	4.4	12
106	Chrysophanol attenuated isoproterenolâ€induced cardiac hypertrophy by inhibiting Janus kinase 2/signal transducer and activator of transcription 3 signaling pathway. Cell Biology International, 2019, 43, 695-705.	3.0	11
107	Poly(ADPâ€ribose) polymerase 1 induces cardiac fibrosis by mediating mammalian target of rapamycin activity. Journal of Cellular Biochemistry, 2019, 120, 4813-4826.	2.6	11
108	Integration of multiscale molecular modeling approaches with the design and discovery of fusidic acid derivatives. Future Medicinal Chemistry, 2019, 11, 1427-1442.	2.3	10

#	Article	IF	CITATIONS
109	In Silico Prediction of Chemical Toxicity Profile Using Local Lazy Learning. Combinatorial Chemistry and High Throughput Screening, 2017, 20, 346-353.	1.1	10
110	Inhalable cryptotanshinone spray-dried swellable microparticles for pulmonary fibrosis therapy by regulating TGF-β1/Smad3, STAT3 and SIRT3 pathways. European Journal of Pharmaceutics and Biopharmaceutics, 2022, 172, 177-192.	4.3	10
111	TIEG1 Inhibits Angiotensin II–induced Cardiomyocyte Hypertrophy by Inhibiting Transcription Factor GATA4. Journal of Cardiovascular Pharmacology, 2015, 66, 196-203.	1.9	9
112	The Use of Gene Ontology Term and KEGG Pathway Enrichment for Analysis of Drug Half-Life. PLoS ONE, 2016, 11, e0165496.	2.5	9
113	Natural product 1,2,3,4,6-penta-O-galloyl-β-D-glucopyranose is a reversible inhibitor of glyceraldehyde 3-phosphate dehydrogenase. Acta Pharmacologica Sinica, 2022, 43, 470-482.	6.1	9
114	Design and synthesis of 28-hydroxy protopanaxadiol as a novel probe template. Natural Product Research, 2017, 31, 1523-1528.	1.8	8
115	Synthesis, antifungal activity and potential mechanism of fusidic acid derivatives possessing amino-terminal groups. Future Medicinal Chemistry, 2020, 12, 763-774.	2.3	8
116	Benzothiazole Amides as TRPC3/6 Inhibitors for Gastric Cancer Treatment. ACS Omega, 2021, 6, 9196-9203.	3.5	8
117	PRMT5 Prevents Cardiomyocyte Hypertrophy via Symmetric Dimethylating HoxA9 and Repressing HoxA9 Expression. Frontiers in Pharmacology, 2020, 11, 600627.	3.5	7
118	Discovery of a novel 53BP1 inhibitor through AlphaScreen-based high-throughput screening. Bioorganic and Medicinal Chemistry, 2021, 34, 116054.	3.0	7
119	The Neuropharmacological Effects of Magnolol and Honokiol: A Review of Signal Pathways and Molecular Mechanisms. Current Molecular Pharmacology, 2023, 16, 161-177.	1.5	7
120	Calcium Signal Pathway is Involved in Prostaglandin E2 Induced Cardiac Fibrosis in Cardiac Fibroblasts. Journal of Pharmacy and Pharmaceutical Sciences, 2018, 21, 326-339.	2.1	5
121	HO-1 nuclear accumulation and interaction with NPM1 protect against stress-induced endothelial senescence independent of its enzymatic activity. Cell Death and Disease, 2021, 12, 738.	6.3	5
122	Relating Substructures and Side Effects of Drugs with Chemical-chemical Interactions. Combinatorial Chemistry and High Throughput Screening, 2020, 23, 285-294.	1.1	5
123	Upregulation of α-enolase protects cardiomyocytes from phenylephrine-induced hypertrophy. Canadian Journal of Physiology and Pharmacology, 2018, 96, 352-358.	1.4	4
124	Analysis of A Drug Target-based Classification System using Molecular Descriptors. Combinatorial Chemistry and High Throughput Screening, 2016, 19, 129-135.	1.1	4
125	The cross-talk between PARylation and SUMOylation in C/EBPβ at K134 site participates in pathological cardiac hypertrophy. International Journal of Biological Sciences, 2022, 18, 783-799.	6.4	4
126	Direct Electrodeposition of Bimetallic Nanostructures on Co-Based MOFs for Electrochemical Sensing of Hydrogen Peroxide. Frontiers in Chemistry, 2022, 10, 856003.	3.6	4

#	Article	IF	CITATIONS
127	Biodegradation Kinetics of Phenanthrene by a Fusant Strain. Current Microbiology, 2012, 65, 225-230.	2.2	3
128	Receptor-interacting protein 140 overexpression impairs cardiac mitochondrial function and accelerates the transition to heart failure in chronically infarcted rats. Translational Research, 2017, 180, 91-102.e1.	5.0	3
129	PEX5 prevents cardiomyocyte hypertrophy via suppressing the redox-sensitive signaling pathways MAPKs and STAT3. European Journal of Pharmacology, 2021, 906, 174283.	3.5	3
130	A novel phosphodiesterase 9A inhibitor LW33 protects against ischemic stroke through the cGMP/PKG/CREB pathway. European Journal of Pharmacology, 2022, 925, 174987.	3.5	3
131	Epigenetic Reader Bromodomain Containing Protein 2 Facilitates Pathological Cardiac Hypertrophy via Regulating the Expression of Citrate Cycle Genes. Frontiers in Pharmacology, 2022, 13, .	3.5	3
132	Analysis of Four Types of Leukemia Using Gene Ontology Term and Kyoto Encyclopedia of Genes and Genomes Pathway Enrichment Scores. Combinatorial Chemistry and High Throughput Screening, 2020, 23, 295-303.	1.1	2
133	A computational method for the identification of candidate drugs for non-small cell lung cancer. PLoS ONE, 2017, 12, e0183411.	2.5	1
134	PKC-ζ Aggravates Doxorubicin-Induced Cardiotoxicity by Inhibiting Wnt/β-Catenin Signaling. Frontiers in Pharmacology, 2022, 13, 798436.	3.5	1
135	Identifying Candidates for Breast Cancer using Interactions of Chemicals and Proteins. Combinatorial Chemistry and High Throughput Screening, 2018, 20, 850-860.	1.1	0
136	9-Cyclopropylmethoxy-dihydrotetrabenazine and its stereoisomers as vesicular monoamine transporter-2 inhibitors. Future Medicinal Chemistry, 2022, 14, 991-1003.	2.3	0